Symmetry and Subunit Arrangement of Tobacco Necrosis Virus (TNV)

By Tomitake Tsukihara, Yukio Yokota* and Takayuki Koyama

Faculty of Engineering, Tottori University, Tottori 680, Japan

and Keiichi Fukuyama and Hiroshi Matsubara

Department of Biology, Faculty of Science, Osaka University, Toyonaka 560, Japan

Abstract

X-ray intensity data for tobacco necrosis virus were obtained at 8 Å resolution using a Weissenberg camera with a large cassette of 430 mm radius. The synchrotron radiation source at the Photon Factory was used. The icosahedral symmetry of the virus as well as its packing in the unit cell were scrutinized by a rotation function. Assuming the subunit to be spherical, its arrangement on the icosahedral surface was determined by an R-factor search at 30 Å resolution. The virus was found to be similar to southern bean mosaic virus in its subunit arrangement. The R factor obtained by merging equivalent reflections was 0·136 for 15 929 reflections with $I > 5\sigma(I)$ and 0·141 for 22 622 reflections with $I > \sigma(I)$.

Introduction

Tobacco necrosis virus (TNV) is a small spherical virus about 280 Å in diameter (Smith & Bald, 1934). It consists of 180 copies of coat protein and a single-stranded RNA with a molecular weight of about $1·3 \times 10^6$. It has been isolated together with its satellite virus, satellite tobacco necrosis virus (STNV). STNV, about 200 Å in diameter, consists of 60 copies of coat protein with a single-stranded RNA, and its crystal structure has been determined at 2·5 Å resolution (Jones & Liljas, 1984). STNV can only multiply with the assistance of its helper, TNV; thus the functional and structural relationships between TNV and STNV are important from a virological viewpoint.

An electron microscopic study (Matthews, 1979) suggests that the 180 copies of TNV coat protein are arranged in $T = 3$ icosahedral symmetry. Various molecular weights ranging from 22 600 to 33 000 have been reported for the coat proteins of the different strains of TNV (Uyemoto & Grogan, 1969; Lesnaw & Reichmann, 1969). In a previous study (Fukuyama, Hirota & Tsukihara, 1987) we obtained

---

* Present address: Department of Biology, Faculty of Science, Osaka University, Toyonaka 560, Japan.

a molecular weight of 30 000 for the coat protein of the present virus. The virus was successfully crystallized, the crystal belonging to the cubic space group $P4_232$ with the cell dimensions, $a = b = c = 338$ Å. In the present study we collected X-ray diffraction data for the TNV crystal, and calculated its self-rotation function in order to confirm the $T = 3$ icosahedral symmetry of the virus and to locate the virus particles in the unit cell. An R-factor search was carried out to determine the arrangement of the 180 copies of coat protein on the virus surface.

Intensity data collection

X-ray data collection, at 2·5 GeV, was carried out at the BL6A2 station at the Photon Factory. The X-ray beam was monochromatized to 1·488 Å by a Si(111) monochromator system. The camera was a screenless Weissenberg camera (Sakabe, 1983) with a cylindrical cassette of 430 mm radius. A crystal measuring $0·5 \times 0·5 \times 0·5$ mm was mounted in a capillary in such a way that it could be rotated about the [111] axis. The total oscillation range of 31·5° was covered by 21 serial Weissenberg photographs, each with an oscillation angle of 1·62°. Individual oscillation ranges overlapped adjacent ones by 0·12°. The exposure period of each scan was 65 s. The crystal was translated after every seven or eight scans to avoid deterioration of the diffraction pattern. The diffraction intensities were recorded on a 400 × 200 mm imaging plate (Fuji Film Co. Ltd). The plates were digitized at 100 μm intervals on a Fuji BA100 read-out system, and the intensity data to 8 Å resolution were processed using the *WEIS* program system (Higashi, 1989). The mosaic spread of each data set was assigned to 0·1°. Intensities of individual plates were scaled by the method of Hamilton, Rollett & Sparks (1965) for 32 713 reflections with $I > 5\sigma(I)$. Statistics of the reflections collected as well as the results of scaling are given in Table 1. The merging R factor is 0·136 for 15 929 reflections with $I > 5\sigma(I)$ and 0·141 for 22 622 reflections with $I > \sigma(I)$. The number of observed independent reflec-

Table 1. *Data-collection statistics*

Film No.	Oscillation range (°)	Collected reflections No. accepted	R.m.s.* DR	R.m.s.* DS	Scaled reflections with $I > 5\sigma(I)$ No.	R
1	−8·00−−6·38	1068	0·64	0·60	770	0·136
2	−6·40−−4·88	1512	0·61	0·54	892	0·135
3	−5·00−−3·88	1593	0·32	0·28	1011	0·128
4	−3·50−−1·88	1452	0·19	0·12	945	0·128
5	−2·00−−0·38	1508	0·38	0·37	956	0·147
6	−0·50−1·12	1560	0·55	0·48	992	0·138
7	1·00−2·62	1557	0·54	0·47	993	0·136
8	2·50−4·12	1233	0·56	0·49	906	0·132
9	4·00−5·62	1773	0·34	0·25	1229	0·106
10	5·50−7·12	1835	0·32	0·22	1278	0·114
11	7·00−8·62	1832	0·28	0·21	1277	0·107
12	8·50−10·12	1882	0·23	0·18	1314	0·104
13	10·00−11·62	1891	0·39	0·21	1307	0·112
14	11·50−13·12	1965	0·47	0·43	1303	0·117
15	13·00−14·62	2002	0·43	0·39	1334	0·115
16	14·50−16·12	1647	0·31	0·26	710	0·206
17	16·00−17·62	1092	0·47	0·34	506	0·178
18	17·50−19·12	509	0·52	0·39	416	0·166
19	19·00−20·62	1609	0·32	0·31	641	0·183
20	20·50−22·62	1605	0·25	0·14	629	0·186
21	22·00−23·62	1588	0·32	0·21	588	0·194
Total		32713			20000	0·136

* R.m.s. in raster step. The definitions of DS and DR are the same as in Higashi (1989).

Table 2. *Independent reflections in each shell*

Resolution (Å)	Theoretical	$F > \sigma(F)$	Observed $F > 3\sigma(F)$	$F > 5\sigma(F)$
100–30	182	151	151	142
30–25	120	102	101	93
25–20	253	215	212	195
20–15	689	522	510	422
15–14	266	194	188	145
14–13	350	250	245	194
13–12	471	358	350	287
12–11	658	544	533	479
11–10	939	764	748	667
10–9	1380	1137	1119	978
9–8	2150	1574	1539	1251
Total	7458	5811	5696	4853

tions and the theoretical value in each shell are listed in Table 2.

Orientation and location of virus particles in the unit cell

For a unit cell of $3·86 \times 10^7$ Å^3, containing two viruses with a molecular weight of about $6·7 \times 10^6$ and located at the Wyckoff position a (*International Tables for Crystallography*, 1983, Vol. A, pp. 626–628), the V_m value (Matthews, 1968) is 2·9 Å^3 per dalton. This seems reasonable by comparison with the corresponding values for crystals of small spherical viruses: 3·5 for belladonna mottle virus (Heuss, Mohana Rao & Argos, 1981); 3·3 for cowpea chlorotic mottle virus (Rayment, Argos & Johnson, 1977); 3·0 for tomato bushy stunt virus (Olson, Bricogne & Harrison, 1983); 2·8 for STNV (Liljas, Unge, Jones, Fridborg, Lovgren, Skoglund & Strandberg, 1982); 2·6 for human rhinovirus-14 (Rossmann, Arnold, Erickson, Frankenberger, Griffith, Hecht, Johnson, Kamer, Luo, Mosser, Rueckert, Sherry & Vriend, 1985); and 2·2 Å^3 per

dalton for Mengo virus (Luo, Vriend, Kamer, Minor, Arnold, Rossmann, Boege, Scrabe, Duke & Palmenberg, 1987). Since the number of icosahedral equivalent points is 60, two virus particles in the unit cell have 120 icosahedral asymmetric units. The space group $P4_232$ has 24 crystallographic asymmetric units, thus five icosahedral asymmetric units related by an icosahedral fivefold symmetry are contained in the crystallographic asymmetric unit. The two particles at the origin (P1) and the body center (P2) are related to each other by the crystallographic 4_2 operation at $(\frac{1}{2},0,z)$. The other crystallographic symmetries of the two- and threefold axes coincide with the respective icosahedral two- and threefold axes of the particle. The unique location and orientation of the virus particles in the unit cell are shown in Fig. 1.

Rotation function calculation

A self-rotation function (Rossmann & Blow, 1962) was computed using the fast-rotation function pro-
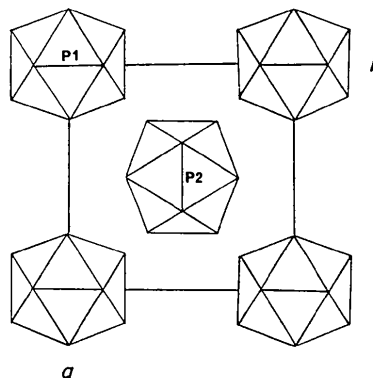
Fig. 1. Orientation and packing of the icosahedral virus particles of TNV in the unit cell for the space group $P4_232$. The crystallographic two- and threefold axes coincide with the respective icosahedral two- and threefold axes. The particle at the origin (P 1) is related to that at the body center (P2) by a 4_2 axis.
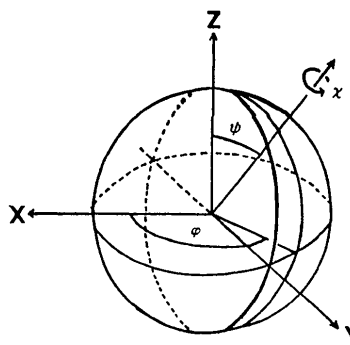
Fig. 2. The polar angles and the orthogonal coordinates used in the calculation of the rotation function. X, Y and Z are parallel to the crystallographic a, b and c axes, respectively.

gram written by Crowther (1972) in order to confirm the symmetry and orientation of the virus in the unit cell. A total of 1281 independent reflections with $F >$ $3\sigma(F)$ between 10 and 12 Å were used in the calculation. The radius of integration was 58 Å and the

maximum value of the function was normalized to 50. The rotation function, obtained in equal Eulerian angles of interval 5°, was transformed to a polar coordinate system (Fig. 2), where the orthogonal axes of X, Y and Z are parallel to the respective
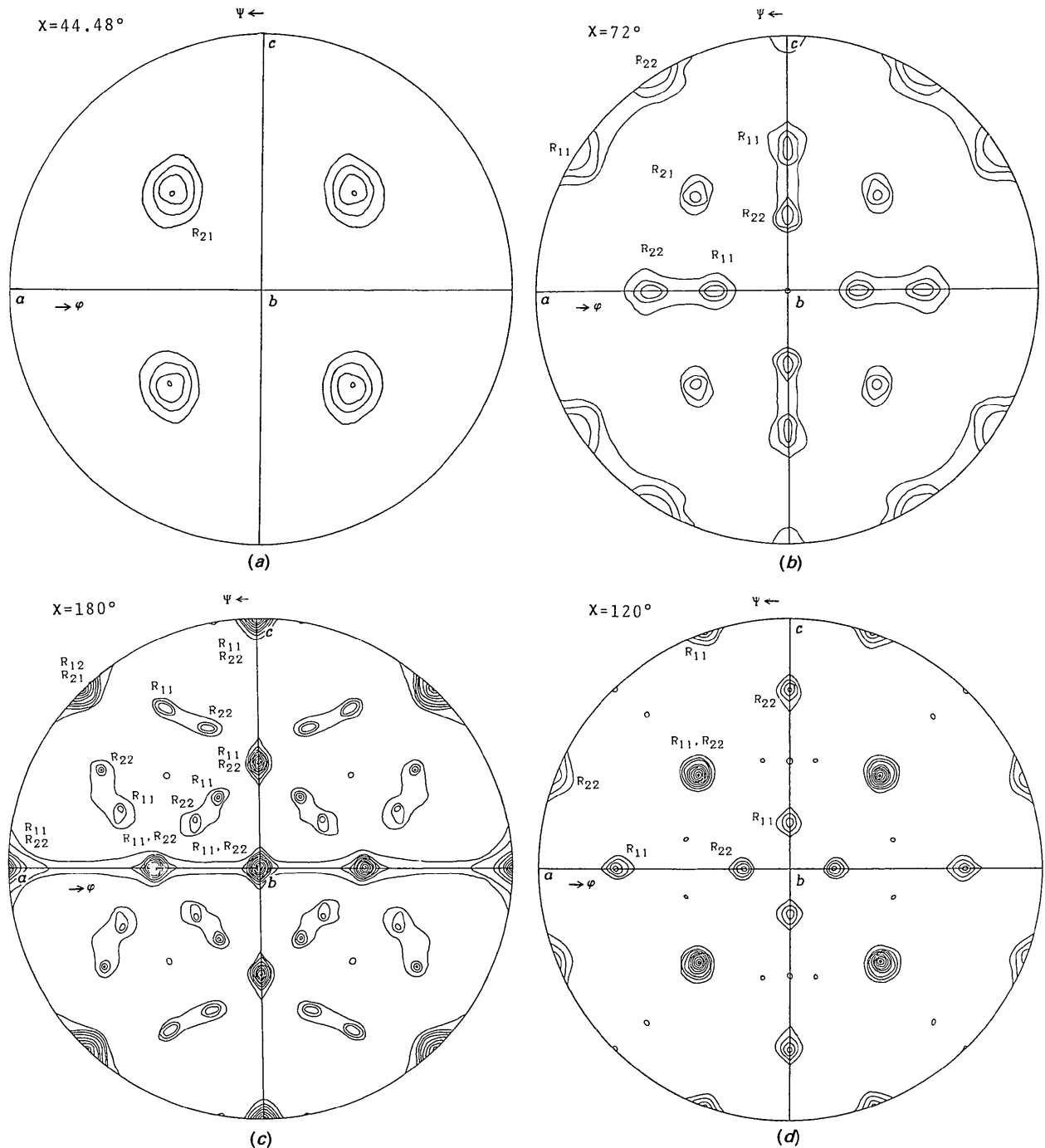
Fig. 3. Stereographic projections of the rotation function. The sections at (a) $\chi = 44\cdot48$, (b) 72, (c) 120 and (d) 180° are given. The maximum peak is normalized to 50. Contours are drawn at equal intervals of five beginning with five. R_{ij}'s indicate types of rotation (see text).

Table 3. Peaks of the rotation function

Rotations*				Heights	Weights
R_{21}	44·48	54·74	45·00	21	single
R_{22}	72·00	31·72	0·00	20	single
R_{11}	72·00	31·72	90·00	21	single
R_{11}	72·00	58·28	0·00	21	single
R_{22}	72·00	58·28	90·00	21	single
R_{22}	72·00	90·00	31·72	19	single
R_{11}	72·00	90·00	58·28	20	single
R_{21}	75·52	54·74	45·00	21	single
R_{12},R_{21}	90·00	0·00	0·00	50	double
R_{12},R_{21}	90·00	90·00	0·00	46	double
R_{12},R_{21}	90·00	90·00	90·00	46	double
R_{21}	110·21	45·78	13·28	19	single
R_{21}	110·21	45·78	76·92	20	single
R_{21}	110·21	80·52	45·00	20	single
R_{11}	120·00	20·91	0·00	20	single
R_{22}	120·00	20·91	90·00	21	single
R_{11},R_{22}	120·00	54·74	45·00	46	double
R_{22}	120·00	69·09	0·00	20	single
R_{11}	120·00	69·09	90·00	20	single
R_{11}	120·00	90·00	20·91	21	single
R_{22}	120·00	90·00	69·09	21	single
R_{21}	138·59	32·31	45·00	21	single
R_{21}	138·59	67·79	24·09	21	single
R_{21}	138·59	67·79	65·91	21	single
R_{22}	144·00	31·72	0·00	21	single
R_{11}	144·00	31·72	90·00	21	single
R_{11}	144·00	58·28	0·00	20	single
R_{22}	144·00	58·28	90·00	20	single
R_{22}	144·00	90·00	31·72	21	single
R_{11}	144·00	90·00	58·28	21	single
R_{21}	154·76	18·46	45·00	21	single
R_{21}	154·76	77·06	13·28	21	single
R_{21}	154·76	77·06	76·72	21	single
R_{21}	164·48	54·74	45·00	20	single
R_{11},R_{22}	180·00	0·00	0·00	50	double
R_{11}	180·00	36·00	31·72	20	single
R_{22}	180·00	36·00	58·28	20	single
R_{12},R_{21}	180·00	45·00	0·00	45	double
R_{11},R_{22}	180·00	45·00	90·00	46	double
R_{22}	180·00	60·00	20·91	21	single
R_{11}	180·00	60·00	69·09	21	single
R_{11}	180·00	72·00	31·72	21	single
R_{22}	180·00	72·00	58·28	21	single
R_{11},R_{22}	180·00	90·00	0·00	50	double
R_{11},R_{22}	180·00	90·00	45·00	50	double
R_{11},R_{22}	180·00	90·00	90·00	50	double

*R_{ii} represents a rotational symmetry element within each individual particle and R_{ij} relates the two individual particles (P_i and P_j) in a similar manner.

crystallographic axes of a, b and c. Stereographic projection of the rotation functions for $\chi = 44\cdot48$, 72, 120 and 180° are shown in Fig. 3.

The rotation function contains peaks arising from rotational symmetry elements within each individual particle (P1 or P2) in the cell together with peaks resulting from rotational symmetry elements which relate the two individual particles (P1 and P2). Here the former peaks are denoted by R_{ii} and the latter by R_{ij}. The rotation function of the present crystal consists of R_{11}, R_{22}, R_{12} and R_{21}, each of which is attributed to 60 rotational operations as in the case of STNV (Litvin, 1975). The angular positions in the polar coordinate system and the multiplicities of peaks were estimated in the range $\chi = 0$ to 180°, $\varphi = 0$ to 90° and $\psi = 0$ to 90°, and are given in Table 3. The maximum noise level was six. Peak heights for R_{11}, R_{22}, R_{12} and R_{21} were 19 to 21 (single) and 45 to 50 (double). Consequently, the icosahedral symmetry and the location of the viruses in the crystal were confirmed.

Determination of subunit arrangement

In order to locate the subunits in the icosahedral asymmetric unit, the R factor was calculated for reflections with spacing 100–30 Å for each assumed position of the subunit. A spherical model 30 Å in diameter with uniform electron density was moved in the shell at a distance of 100–140 Å from the center of the virus particle. We assumed a quasi (local) threefold axis in the icosahedral asymmetric unit; the local threefold axis was fixed along the normal of an equilateral triangle the vertices of which were located on the icosahedral five- or threefold axes and at 169 Å from the center of the virus particle. The local threefold axis and the equilateral triangle are depicted in Fig. 4. Contours of the R-factor map were drawn at equal intervals of -5% starting from 70% (Fig. 5). This results in mirror symmetry in addition to the icosahedral symmetries, since the subunit is assumed to be spherical and the local threefold axis is located on a bisecting plane of the trigonal pyramid of the icosahedral asymmetric unit. The spherical subunit is uniquely located in the R map at $(-15\cdot0, 14\cdot1, 130\cdot5)$ or $(15\cdot0, 14\cdot1, 130\cdot5)$ in an orthogonal coordinate system (Fig. 5), and these positions are related to each other by mirror symmetry. The subunit arrangement on the icosahedral surface is shown by the stereoscopic view in Fig. 6(a).

Concluding remarks

The icosahedral symmetry of the virus as well as its packing in the unit cell have been established by the rotation function. The centers of the three subunits related to each other by the local threefold axis lie at 132, 136 and 144 Å from the center of the virus particle. The virus protrudes out to 158·8 Å along the fivefold axes. The virus particles do not overlap each other in the unit cell. The subunits, which are
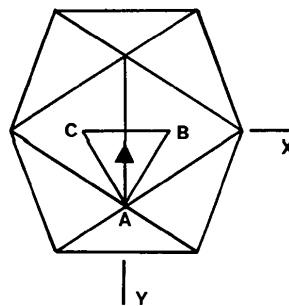
Fig. 4. The presumed local threefold axis (▲) is the normal of the equilateral triangle of ABC at its center. A lies on a fivefold axis, and B and C on threefold axes. They lie at a distance of 169 Å from the center of the particle. The trigonal pyramid made up of A, B, C and the center of the virus is the icosahedral asymmetric unit.

30 Å in diameter, pack with a small overlap and a small vacancy on the icosahedral surface. The SBMV structure (Fig. 6b) is shown as spherical subunits 30 Å in diameter at the respective centers of gravity
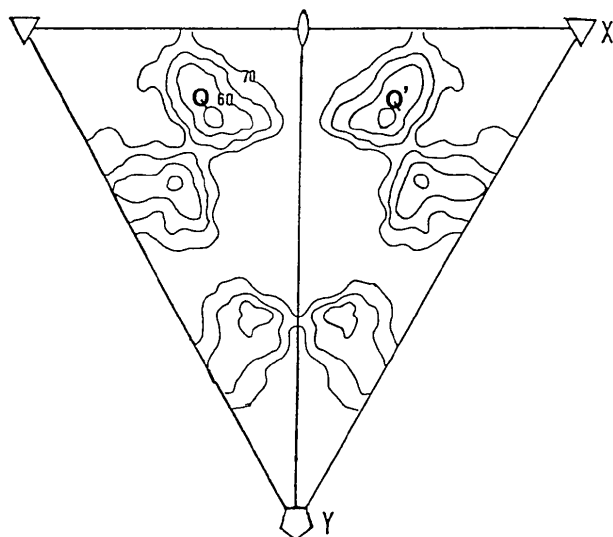
Fig. 5. R-factor map for the section $Z = 129\cdot6$ Å. Contours are drawn at equal intervals of -5% beginning with 70%. The values at $Q(-15\cdot0, 14\cdot1)$ and $Q'(15\cdot0, 14\cdot1)$ are the minima in this section. The other sites exhibiting a local minimum are related to Q or Q' by the local threefold axis.

(a)

(b)
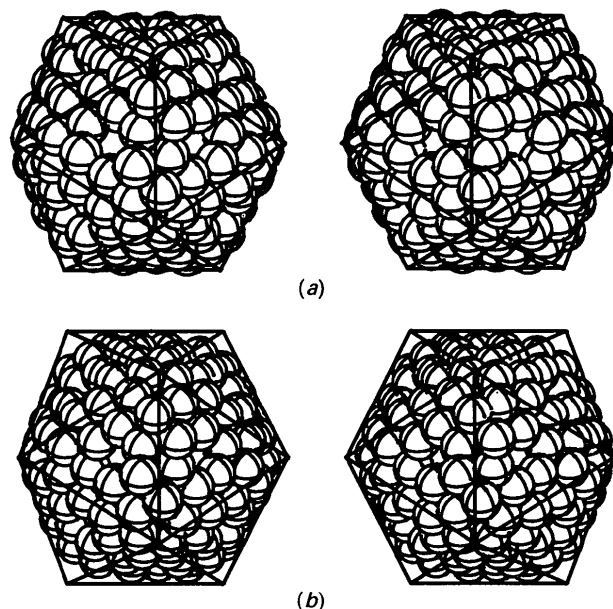
Fig. 6. Stereoscopic drawings of (a) TNV and (b) SBMV. The subunits, with spheres 30 Å in diameter, are drawn in the icosahedral lattice. The viruses are viewed downward from a twofold axis. Both viruses show a similar arrangement.

obtained from the Protein Data Bank (Abad-Zapatero, Abdel-Meguid, Johnson, Leslie, Rayment, Rossmann, Suck & Tsukihara, 1981; Bernstein, Koetzle, Williams, Meyer, Brice, Rodgers, Kennard, Shimanouchi & Tasumi, 1977). Comparing the two structures in Figs. 6(a) and 6(b), it can be seen that TNV resembles SBMV in the arrangement of its subunits.

References

ABAD-ZAPATERO, C., ABDEL-MEGUID, S. S., JOHNSON, J. E., LESLIE, A. G. W., RAYMENT, I., ROSSMANN, M. G., SUCK, D. & TSUKIHARA, T. (1981). Acta Cryst. B37, 2002–2018.
BERNSTEIN, F. C., KOETZLE, T. F., WILLIAMS, G. J. B., MEYER, E. F. JR, BRICE, M. D., RODGERS, J. R., KENNARD, O., SHIMANOUCHI, T. & TASUMI, M. (1977). J. Mol. Biol. 112, 535–542.
CROWTHER, R. A. (1972). The Molecular Replacement Method, edited by M. G. ROSSMANN, pp. 173–178. New York: Gordon & Breach.
FUKUYAMA, K., HIROTA, S. & TSUKIHARA, T. (1987). J. Mol. Biol. 196, 961–962.
HAMILTON, W. C., ROLLETT, J. S. & SPARKS, R. A. (1965). Acta Cryst. 18, 129–130.
HEUSS, K. L., MOHANA RAO, J. K. & ARGOS, P. (1981). J. Mol. Biol. 146, 629–633.
HIGASHI, T. (1989). J. Appl. Cryst. 22, 9–18.
JONES, T. A. & LILJAS, L. (1984). J. Mol. Biol. 177, 735–767.
LESNAW, J. A. & REICHMANN, M. E. (1969). Virology, 39, 729–737.
LILJAS, L., UNGE, T., JONES, T. A., FRIDBORG, K., LOVGREN, S., SKOGLUND, U. & STRANDBERG, B. (1982). J. Mol. Biol. 159, 93–108.
LITVIN, D. B. (1975). Acta Cryst. A31, 407–416.
LUO, M., VRIEND, G., KAMER, G., MINOR, I., ARNOLD, E., ROSSMANN, M. G., BOEGE, U., SCRABE, D. G., DUKE, G. M. & PALMENBERG, A. C. (1987). Science, 235, 182–191.
MATTHEWS, B. W. (1968). J. Mol. Biol. 33, 491–497.
MATTHEWS, R. E. F. (1979). Intervirology, 12, 252.
OLSON, A. J., BRICOGNE, G. & HARRISON, S. C. (1983). J. Mol. Biol. 171, 61–93.
RAYMENT, I., ARGOS, P. & JOHNSON, J. E. (1977). J. Ultrastruct. Res. 61, 240–242.

Rossmann, M. G., Arnold, E., Erickson, J. W., Franken-berger, E. A., Griffith, J. P., Hecht, H.-J., Johnson, J. E., Kramer, G., Luo, M., Mosser, A. G., Rueckert, R. R., Sherry, B. & Vriend, G. (1985). *Nature* (*London*), **317**, 145–153.

Rossmann, M. G. & Blow, D. M. (1962). *Acta Cryst.* **15**, 24–31.

Sakabe, N. (1983). *J. Appl. Cryst.* **16**, 542–547.

Smith, K. M. & Bald, J. G. (1934). *Parasitology*, **27**, 231–253.

Uyemoto, J. K. & Grogan, R. G. (1969). *Virology*, **39**, 79–89.

Structure and Conformational Features of 9-(4-Diethylaminophenyl)acridine

By Stephen Neidle,* Mavis Agbandje, Terence C. Jenkins and Adrian W. McConnaughie

Cancer Research Campaign Biomolecular Structure Unit, Institute of Cancer Research, Cotswold Road, Sutton, Surrey SM2 5NG, England

Abstract

$C_{23}H_{22}N_2$, $M_r = 326.44$, triclinic, $P\bar{1}$, $a = 10.525$ (7), $b = 10.538$ (9), $c = 9.177$ (2) Å, $\alpha = 105.42$ (5), $\beta = 95.96$ (6), $\gamma = 63.57$ (6)°, $V = 878.5$ Å^3, $Z = 2$, $D_x = 1.234$ Mg m^{-3}, λ(Cu $K\alpha$) = 1.54178 Å, $\mu = 0.52$ mm^{-1}, $F(000) = 348$, $T = 294$ K, final $R = 0.056$ for 1299 observed reflections. The acridine ring is highly planar. The 9-phenyl substituent is oriented [dihedral angle 74.5 (3)°] in a similar manner to the analogous 5-phenyl structures. Extensive molecular-orbital (MNDO) calculations on the model 9-phenylacridine system have confirmed that this geometry is energetically favoured, and have revealed the shape of the energy surface for rotation about the C—C bond connecting the phenyl ring and acridine chromophore.

Introduction

A large number of acridines substituted at the 9-position have been studied with respect to potential DNA-binding affinity and anti-tumour activity (Baguley, Denny, Atwell & Cain, 1981; Baguley & Finlay, 1988). In particular, 9-arylamino substitution has resulted in a number of biologically active and DNA-intercalative compounds, with the 3'-methoxy-4'-methanesulfonanilide derivative ('amsacrine') having outstanding activity.

We have previously shown that direct attachment of a phenyl group to the aromatic acridine chromophore, without an intervening amino linkage, results in compounds that retain DNA-binding activity (Abraham, Neidle & Acheson, 1987; Abraham, Agbandje, Neidle & Acheson, 1988). The present paper extends this type of linkage to the 9-position.

---

* Address correspondence to this author.

In particular, we examine the conformational properties of the 9-phenylacridine series with respect to the linking C—C bond.

Experimental

The title compound was synthesized by reflux condensation of 9(10H)-acridone, phosphoryl chloride and N,N-diethylaniline using a literature procedure (Albert, 1966). Recrystallization from petroleum (313–333 K fraction) afforded brownish-yellow plates, m.p. 470.5–471 K (literature 470 K). A crystal of dimensions $0.20 \times 0.20 \times 0.15$ mm was used. The space group was $P\bar{1}$ (No. 2, triclinic). Cell dimensions were obtained from least-squares refinement of 25 2θ values measured on an Enraf–Nonius CAD-4 diffractometer; graphite-monochromated Cu $K\alpha$ radiation ($\lambda = 1.54178$ Å) was used. Intensity data were collected using an ω–2θ scan technique and a maximum scan time of 120 s per reflection, for $1.5 \le \theta \le 60.0°$ and $-13 \le h \le 13$, $-17 \le k \le 17$, $0 \le l \le 11$; 2603 unique reflections were measured of which 1299 had $I \ge 2\sigma(I)$. Three intensity standard reflections were monitored every 200 reflections of X-ray exposure during the data collection and showed no statistically significant crystal decay. An empirical *DIFABS* absorption correction was applied (Walker & Stuart, 1983); minimum and maximum absorption correction factors of 0.91 and 1.15, respectively, were used. The structure was solved by direct methods with *MULTAN*82 (Main *et al.*, 1982) and refined by full-matrix least-squares techniques on F. H-atom positions were generated from geometric considerations and were kept fixed during the refinement. The final R was 0.056 and wR was 0.064 with $w = 1/[\sigma^2(F) + 0.04(F)^2]$. The maximum Δ/σ was 0.01 and the e.s.d. of observation of unit weight was 1.81; the maximum and minimum electron density levels in